Separation & Purification Reviews
Publication details, including instructions for authors and subscription information:
http://www.informaworld.com/smpp/title~content=t713597294

Cycling Zone Separations

P. C. Wankat[a]; J. C. Dore[a]; W. C. Nelson[a]
[a] Department of Chemical Engineering, Purdue University, West Lafayette, IN

To cite this Article Wankat, P. C. , Dore, J. C. and Nelson, W. C.(1975) 'Cycling Zone Separations', Separation & Purification Reviews, 4: 2, 215 — 266
To link to this Article: DOI: 10.1080/03602547508066041
URL: http://dx.doi.org/10.1080/03602547508066041

SEPARATION AND PURIFICATION METHODS, 4(2), 215-266 (1975)

CYCLING ZONE SEPARATIONS

P.C. Wankat, J.C. Dore, and W.C. Nelson
Department of Chemical Engineering
Purdue University, West Lafayette, IN 47907

SUMMARY

This article discusses cycling zone separations for the reader not already familiar with cyclic separations. Two models, the counter-current distribution model and the local equilibrium model, are developed in depth and used to explain and predict both single component and multi-component separations. Both the direct mode and traveling wave mode of operation are treated. Experimental results utilizing both temperature and concentration as thermodynamic variables are presented and compared with theoretical predictions for single component separations. Conditions for good separations in both single component and multi-component systems are outlined. Some of the experimental results have not been previously presented.

INTRODUCTION

Recently, there has been considerable interest in cyclic separation processes which allow for continuous or semi-continuous feed to chromatographic or adsorption systems. These processes such as pressure-swing adsorption, parametric pumping, and cycling zone adsorption utilize the periodic variation of a thermodynamic variable to force the separation while feed is added continuously or semi-continuously instead of as a pulse as is common in standard elution.

The first cyclic separation processes were developed in the late 1950's. In 1959, Skarstrom[1] invented the process called heatless adsorption or pressure-swing adsorption. In this technique adsorption of solute from a gas stream was done at a high pressure and desorption was done at low pressures. Thus, at high mass flow rates the solute was held up and the exit gas was purified. At low mass flow rates the bed could be purged since the solute was released.

For the separation of liquids, pressure changes have only a small effect on the distribution coefficients. However, a large effect can be produced by using temperature changes. In 1966, a cyclic process for liquid separation called parametric pumping was developed by Wilhelm and his coworkers.[2] In this technique the fluid to be separated was pumped up through a solid stationary adsorbent into a reservoir and then down through the bed into a second reservoir. This cycle was repeated. In the original mode of operation the fluid in the upper reservoir was cooled while the fluid in the lower reservoir was heated. Since the adsorbent held solute when the fluid was cool, solute was held as the cold fluid was pumped down to the lower reservoir. Similarly, solute was released when the hot fluid was pumped up to the upper reservoir. Under ideal conditions, eventually all the solute found its way into the upper reservoir and a separation was produced.

In the late 1960's, researchers questioned whether flow reversal was actually necessary for a separation since, as a batch or semi-continuous operation, production rates were limited using parametric pumping. Pigford, et. al.[3] developed an essentially continuous technique called cycling zone adsorption in 1969. In this process the fluid to be separated was pumped in one direction through a series of columns and the technique was applicable for separations involving either gases or liquids. Cycling zone adsorption is the subject of this paper. The other techniques are discussed in a recent review by Wankat.[4]

An intuitive understanding of cycling zone adsorption can be obtained through a brief physical description of the process.

Consider a column packed with a stationary solid adsorbent that retains solute at low temperatures and releases the solute at high temperatures. The solution to be treated is fed continuously to the column using equipment which causes its temperature to vary as a square wave starting with a cold temperature for half the cycle and then switching to a hot temperature for the remainder of the cycle. For the first half cycle, the mobile phase enters at a low temperature and the solute is retained; that is, its velocity through the column is considerably slower than that of the mobile phase. As a result, the exiting fluid will initially have a very low solute concentration. The length of this period of low concentration depends on how strongly the solute is retained. Of course, with long cycle times the exiting solute concentration would rise and finally correspond to the feed concentration much like breakthrough curves in ion-exchange systems. For the last half cycle mobile phase enters at a high temperature. As the fluid flows through the column the adsorbent now releases the solute to the fluid since the temperature is high. Thus, the exiting fluid will initially have a high solute concentration. Again, with long enough cycle times the exiting solute concentration would fall and eventually correspond to the feed concentration. The reason for this is that all the solute previously retained would have been released and the solute would be moving through the column unchanged. If the cycle described above were repeated continuously, it would represent a crude example of cycling zone adsorption. In the case above, temperature is the thermodynamic variable that is varied periodically. For inlet fluid temperature varying periodically, the outlet solute concentration varies periodically. With proper timing, a stream of high solute concentration and a stream of low solute concentration can be obtained with continuous feed.

Theoretically, cycling zone adsorption can be used to separate multi-component mixtures as well as remove single components from a solvent. Possible applications are widespread. Among the systems already investigated with industrial importance are the separation of salt from sea water, the separation of

oxygen from air, and the multi-component separation of glucose and fructose from water. As attention is focused on the world-wide problems of pollution, disease, and malnutrition, cycling zone adsorption could find laboratory and industrial applications in biochemicals, pharmaceuticals, food processing, and waste treatment. A single component separation could be the removal of carcinogens from waste water. Similarly, this technique might find relevance in preparative multi-component biochemical separations.

This paper presents two different theoretical models to explain cycling zone adsorption. These two approaches attempt to provide a basis for predicting the amount of separation possible and character of the outlet concentration waves. The article discusses the different operational modes of the technique and considers thermodynamic variables in addition to temperature for forcing a separation. Experimental results, including those with industrial relevance, are presented and compared with theoretical predictions for single component separations. Conditions for good separations in both single component and multicomponent systems are introduced. The theoretical models and most of the experimental results have appeared previously. New experimental results on removal of a dye from water in a counter-current-distribution apparatus using sodium carbonate concentration as the cyclic variable, and new results on removing sugars from water in a chromatographic apparatus using pH as the cyclic variable are also presented.

EQUILIBRIUM STAGE MODEL

Although cycling zone separation is generally considered a continuous separation, a discrete transfer staged apparatus can be operated in the cycling zone mode. This discrete staged apparatus provides a useful model in explaining various aspects of continuous cycling zone separations, especially zone broading. The staged model is based on the counter-current distribution (CCD)

model of Craig and Craig.[5] CCD has proven a useful technique for the modeling of chromatographic separations, although it has been used mainly as a separation technique in the field of biochemistry. The discrete stage model does not physically represent a continuous separation, but its results apply qualitatively to continuous flow systems. The CCD model has been extensively applied to cycling zone separations by Wankat.[6,7,8]

Figure 1 shows an apparatus of the CCD type which gives a cycling zone separation. The separation may be operated in either the direct or traveling wave mode. In the direct mode, all the stages in a region are held at the same temperature, T_H (hot) or T_C (cold), for the first half of the cycle and are switched for the second half cycle. In the traveling wave mode of operation, the temperature of the feed to each region is varied in a periodic fashion by external heat exchangers. The first system to be considered in detail is direct mode cycling zone extraction.

THE DIRECT MODE

The discrete staged system shown in Figure 1 has n x m stages arranged into m regions with n stages per region. The system is operated in temperature cycles with solute being stored in the stationary phase in regions of low temperature and rejected in regions of high temperature (systems of the opposite type are

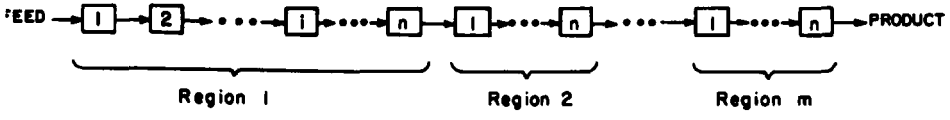

FIGURE 1

Staged Cycling Zone Extraction System for Direct Mode.[6]

certainly possible but are not discussed here for simplicity). A change in temperature causes a change in the equilibrium distribution of solute between the stationary and mobile phase. A given region is operated alternately hot and cold while the following region is operated at the opposite temperature. This alternation of temperatures in time and space causes the solute to be concentrated in half the cycle and depleted in the other half cycle. By synchronizing the period of each cycle (number of transfer steps) with the natural rate of solute movement a maximum separation may be achieved. In addition, an increase in the number of regions should cause an increase in the separation.

The theory for direct mode cycling zone extraction in a staged system is based heavily on the well established theory of counter-current distribution. Each stage shown in Figure 1 is represented by the subscripts (i, j) where i refers to the stage number in region j. The cycles are divided into cycle "halves" (not necessarily equal halves) with S_1 transfers in the first half cycle and S_2 transfers in the second half for a total of S_T transfer steps. The volume of the moving phase in each stage, V_M, and the volume of the stationary phase, V_S, are assumed to be constant. c_M and c_S represent the concentration of the moving and stationary phases respectively. For the present calculation, the distribution coefficient defined as $K(T) = c_M/c_S$ will be a function of temperature but not concentration. The effect of concentration on K(T) could be taken into account through the use of Langmuir adsorption isotherms.[9] Finally, $M_{i,j,s}$ is the mass of solute in stage i of region j, and $f_{i,j,s}$ is the fraction of solute in the moving phase of stage i in region j after transfer step S of the cycle.

It has been shown[5] that the total fraction of solute in the moving phase at equilibrium is given by

$$f_{i,j,s} = \frac{K(T_{i,j,s})\, V_M/V_S}{1 + K(T_{i,j,s})\, V_M/V_S} \qquad (1)$$

The fraction of solute in the stationary phase can be expressed as $1 - f_{i,j,s}$. It is important to note that $f_{i,j,s}$ changes (becomes f_H or f_C) as the temperature varies, unlike CCD machines where $f_{i,j,s}$ and $T_{i,j,s}$ are constant.

Using this relationship, a mass balance can be written to calculate the mass of solute in stage (i,j) after s transfer steps. The mass of solute in stage (i,j) after transfer s is equal to the amount of solute transferred in with the moving phase from stage (i-1,j) plus the amount of solute left behind in the stationary phase of stage (i,j). If $i \neq 1$, this mass balance is

$$M_{i,j,s} = (f_{i-1,j,s-1}) M_{i-1,j,s-1} + (1-f_{i,j,s-1}) M_{i,j,s-1} \quad (2)$$

If $i = 1$ but $j \neq 1$,

$$M_{1,j,s} = (f_{n,j-1,s-1}) M_{n,j,s-1} + (1 - f_{1,j,s-1}) M_{1,j,s-1} \quad (3)$$

Finally, if $i = 1$ and $j = 1$

$$M_{1,1,s} = c_{Feed} V_M + (1 - f_{1,1,s-1}) M_{1,1,s-1} \quad (4)$$

where c_{Feed} is the concentration of solute in the feed. At this point, one would like to know the concentration of product leaving stage (n,m) after each transfer step.

A straightforward solution may be obtained by using equations (2), (3), and (4) as recursion relations with the initial condition of no solute in all the stages. When this is done, an additional subscript is needed in these equations to count the number of cycles. This cycle subscript is not used because the cycling zone system will eventually reach a limiting repeating state, where each cycle is an exact repeat of the cycle before it. This has been shown both experimentally and theoretically. For the study of only the repeating state, a different solution technique may be employed which is discussed in detail elsewhere.[6]

Even with the repeating state assumption, the solution is a function of six variables -- n, m, S_1, S_2, f_H, and f_C. Before moving on to some results for the direct mode system, a qualitative feel for what can be expected would be helpful. The key

factor in this separation is the rate of movement of the solute through the system. Since f is the fraction of solute in the moving phase, the average distance that a solute molecule can move is f x (number of transfer steps). A separation is forced when the temperature is changed and solute is either rejected or stored by the stationary phase. To get the maximum separation each solute molecule should undergo one and only one temperature change in each region.

$$\frac{f \times (\text{number of transfer steps})}{(\text{number of stages region})} = 1 \tag{5}$$

However, f is not constant and varies between the limits f_H and f_C to give the relationship

$$\frac{(\text{number of stages/region})}{f_C} \geq \frac{\text{number of transfers}}{\text{half cycle}} \geq \frac{\text{number of stages/region}}{f_H} \tag{6}$$

This simple argument based on the velocity of solute moving through the system does a good job of predicting the separation behavior. Note that this is essentially the retention argument of chromatography.

To illustrate the application of the direct mode staged system, theoretical and experimental results are presented for the diethylamine - toluene - water system. A separation of diethylamine and water is obtained when the diethylamine selectively distributes between the stationary toluene phase and the moving water phase. The objective is to concentrate the diethylamine in half the water phase and purify the remaining water. The system under study is convenient because there is a large change in the distribution coefficient with temperature and hence very few stages are required. The apparatus used consisted of stoppered glass centrifuge test tubes with the moving phase transferred from stage to stage with a syringe.[6]

The unsteady state solution of equation (2) for the discrete stage model has been programed on a computer. The theoretical results for this model are presented in Figures 2 - 6 and are

compared to experimental results in Figure 7. The optimum number of transfers/half cycle, the effect of the number of transfer steps/half cycle, the effect of changing f_H and f_C, the effect of more regions or more stages/regions, and finally the agreement between theory and experiment were studied.

Figures 2 to 4 show the product concentration over an entire cycle for a system with 5 stages/region, 4 regions, $f_C = .50$, and $f_H = .60$. Symmetric cycles have been used with 10, 17, and 28 transfers per half cycle. The purpose of these plots is to show the importance of timing the concentration waves to enter a region in sequence with heating and cooling. Comparing these figures, 10 transfers per half cycle gives the best separation and 17 the worst. With 10 transfers per half cycle, the natural rate of movement of the solute is sequenced with the changes in temperature of each region, and equation (6) is satisfied. Conversely, at 17 transfers per half cycle, there is a considerable cancellation effect. Figure 4 is interesting since it shows approximately one and one half complete separation waves exiting from the system for each half cycle. It is clear in Figure 2 that the concentration is at a maximum when the product is leaving the hot region.

Figure 5 shows the maximum and minimum product concentration plotted versus the number of transfers/half cycle. This predicts a maximum separation at 10 transfers/half cycle and a minimum separation at 17 transfers/half cycle which is in agreement with Figures 2 and 3. Figures 2, 3, and 4 can be interpreted as having one, two, or three complete waves exiting from the system for each full cycle. With one wave there is maximum separation, with two waves maximum interference, and with three waves some interference and some separation. For a single region device, peak-to-peak separations do not change with the number of transfers/cycle since there is no timing of subsequent regions. However, when the cycle is too long in a single region, some solute molecules pass completely through the region without a

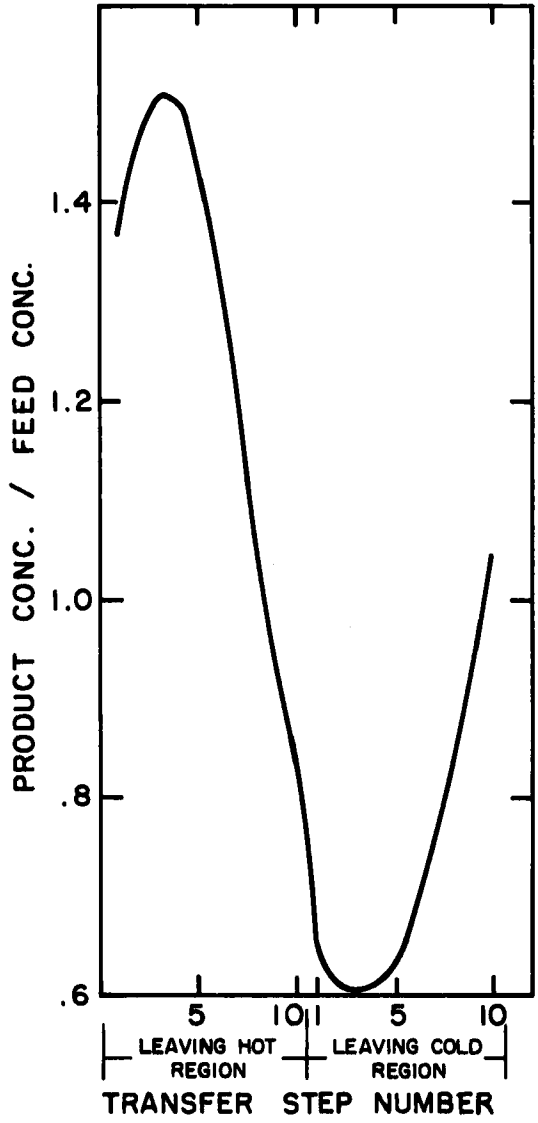

FIGURE 2

Product Concentrations for a Complete Cycle in Direct Mode: 5 stages/region, 4 regions, $f_C = .5$, $f_H = .6$, 10 transfers/half cycle.[6]

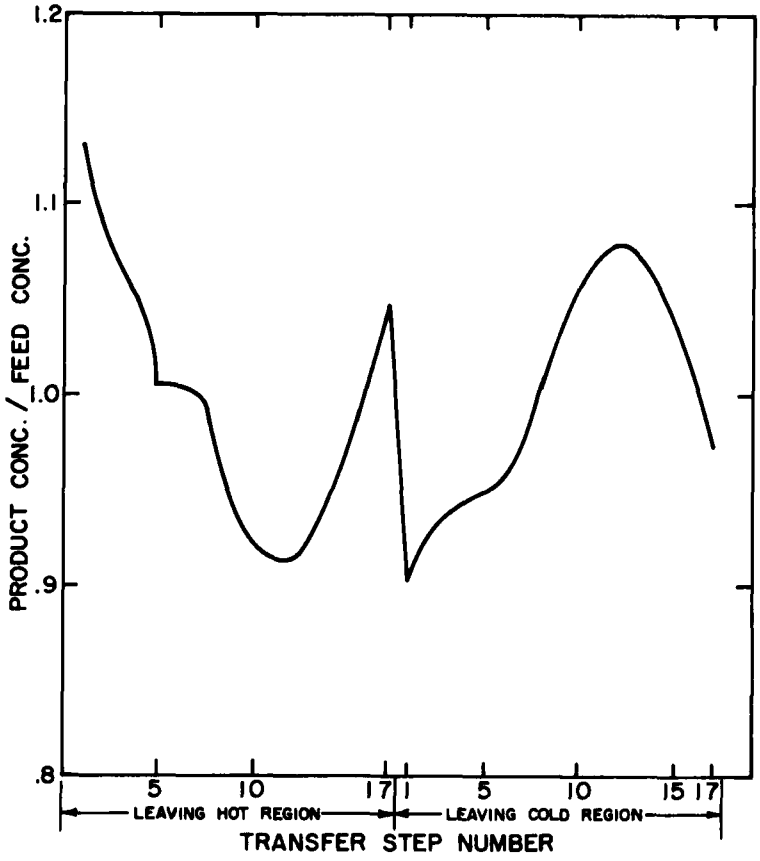

FIGURE 3

Product Concentrations for a Complete Cycle in Direct Mode: 5 stages/region, 4 regions, f_C = .5, f_H = .6, 17 transfers/half cycle.[6]

change in temperature and are not separated. As a result, shoulders appear on the concentration plots and the average separation is decreased. Again the best separation is acheived if equation (6) is satisfied.

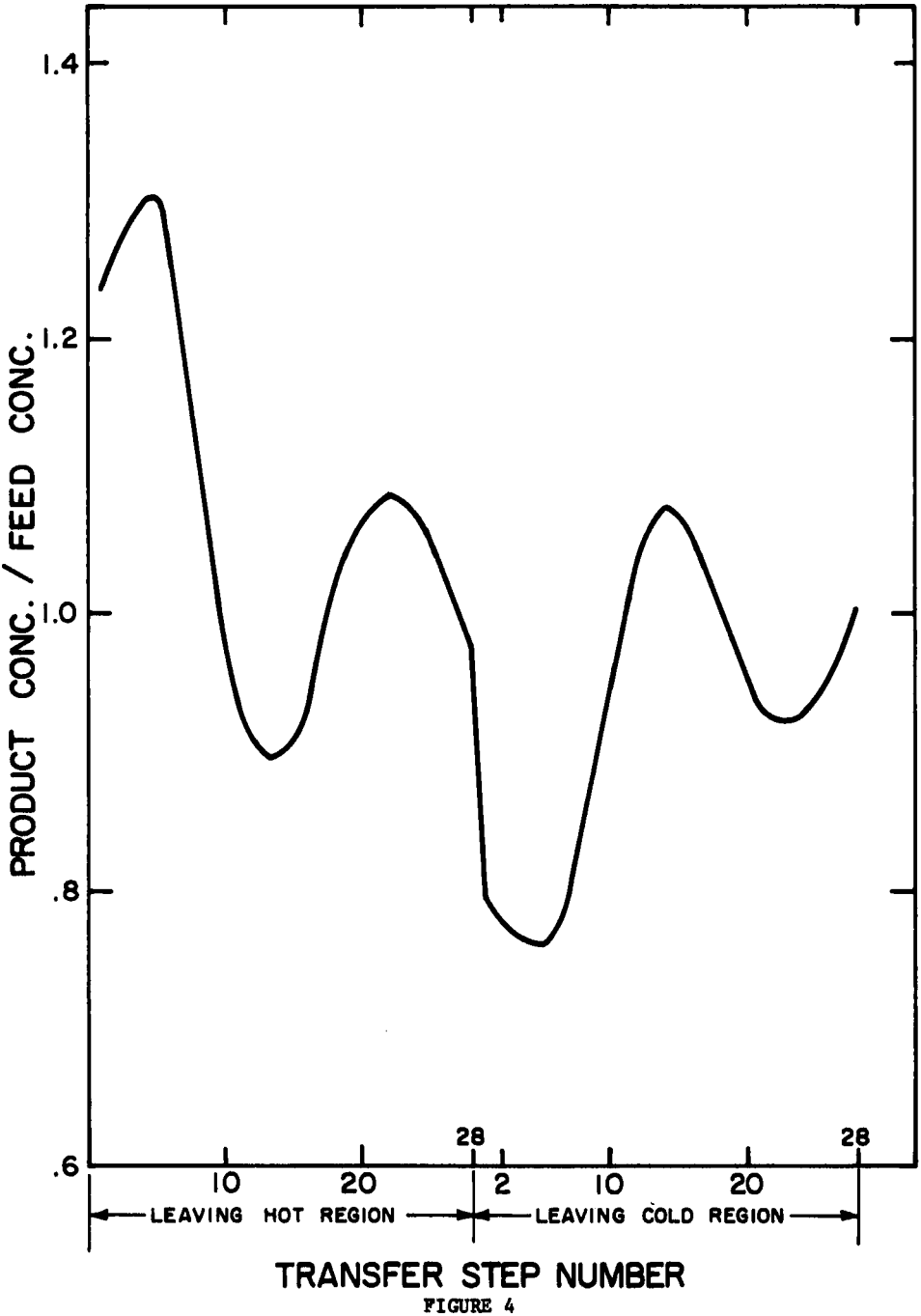

FIGURE 4

Product Concentrations for a Complete Cycle in Direct Mode: 5 stages/region, 4 regions, $f_C = .5$, $f_H = .6$, 28 transfers/half cycle.[6]

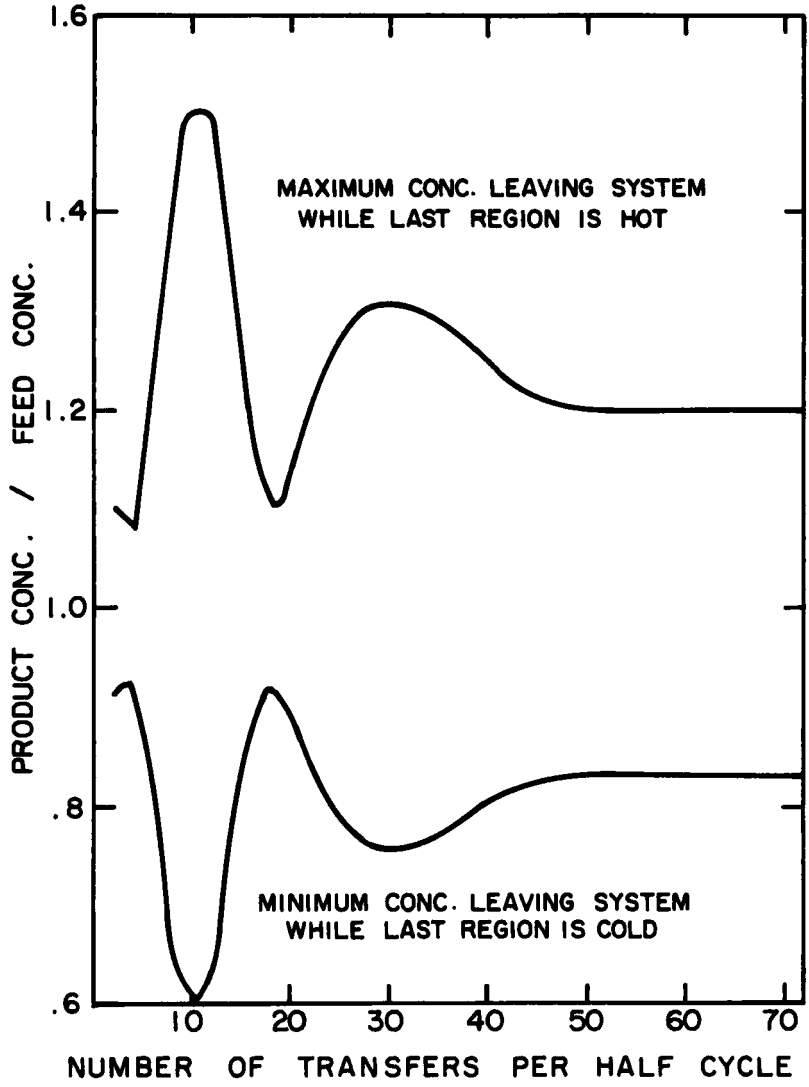

FIGURE 5

Maxima and Minima Product Concentrations as a Function of the Number of Transfers per Half Cycle in Direct Mode: 5 stages/region, 8 regions, $f_C = .5$, $f_H = .6$.[6]

The effect of varying f_C and f_H when $f_H > f_C$ can be seen by comparing Figure 6 to Figure 5. As predicted by equation (6), the maxima and minima are shifted. In addition, there is less separation achieved at the lower f values even though the ratio

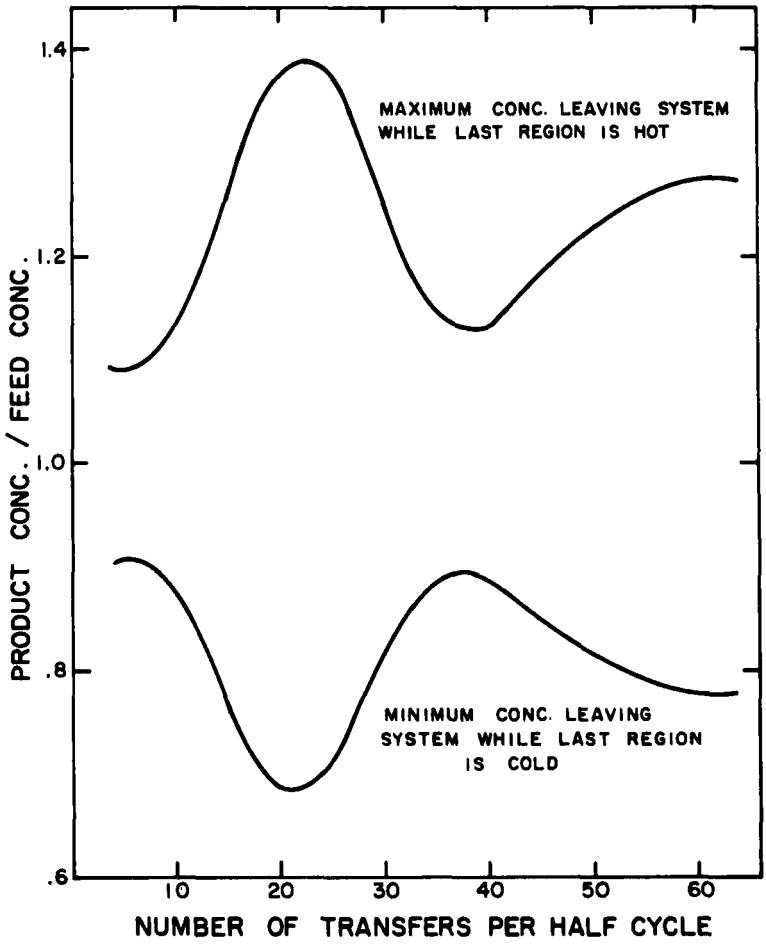

FIGURE 6

Maxima and Minima Product Concentrations as a Function of the Number of Transfers per Half Cycle in Direct Mode: 5 stages/region, 4 regions, $f_C = .25$, $f_H = .3$.[6]

of f_C/f_H remains unchanged. Also, a larger number of transfer steps are required for the optimum separation at low f values.

Results are available indicating the effect of the number of regions and the number of stages/region. Increasing the number of regions increases the separation while having little effect on the location of the maxima and minima. Increasing the number of stages/region both increases separation and changes the location of the maxima and minima. With a fixed number of stages, there is a trade off between the number of stages/region and the number of regions.

A comparison of experimental and theoretical results is shown in Figure 7. The experimental results agree qualitatively with theoretical predictions, except that the concentration jump when the temperature changed was much smaller than predicted. The theoretical results predict a greater separation than was acheived. This difference might be expected since the theoretical model did not account for the non-constant distribution coefficient or the evaporation losses during experimentation. In general, the theory and the probability explanation for rate of movement of solute appear to explain the major effects that occurred.

TRAVELING WAVE MODE

The equilibrium staged system for cycling zone separations can be extended to the traveling wave mode of operation.[7] The basic apparatus for the traveling wave mode, shown in Figure 8, is very similar to that used for the direct mode in Figure 1. The apparatus consists of a series of well insulated equilibrium stages or test tubes arranged into regions with heat exchangers between regions. The feed to the apparatus is of constant composition but its temperature varies as a square wave starting at some hot temperature, T_H, for half the cycle and then switching to the cold temperature, T_C, for the remainder of the cycle. The streams coming from region 1 may be taken as products, or they may be fed to a heat exchanger and then to a second region. The

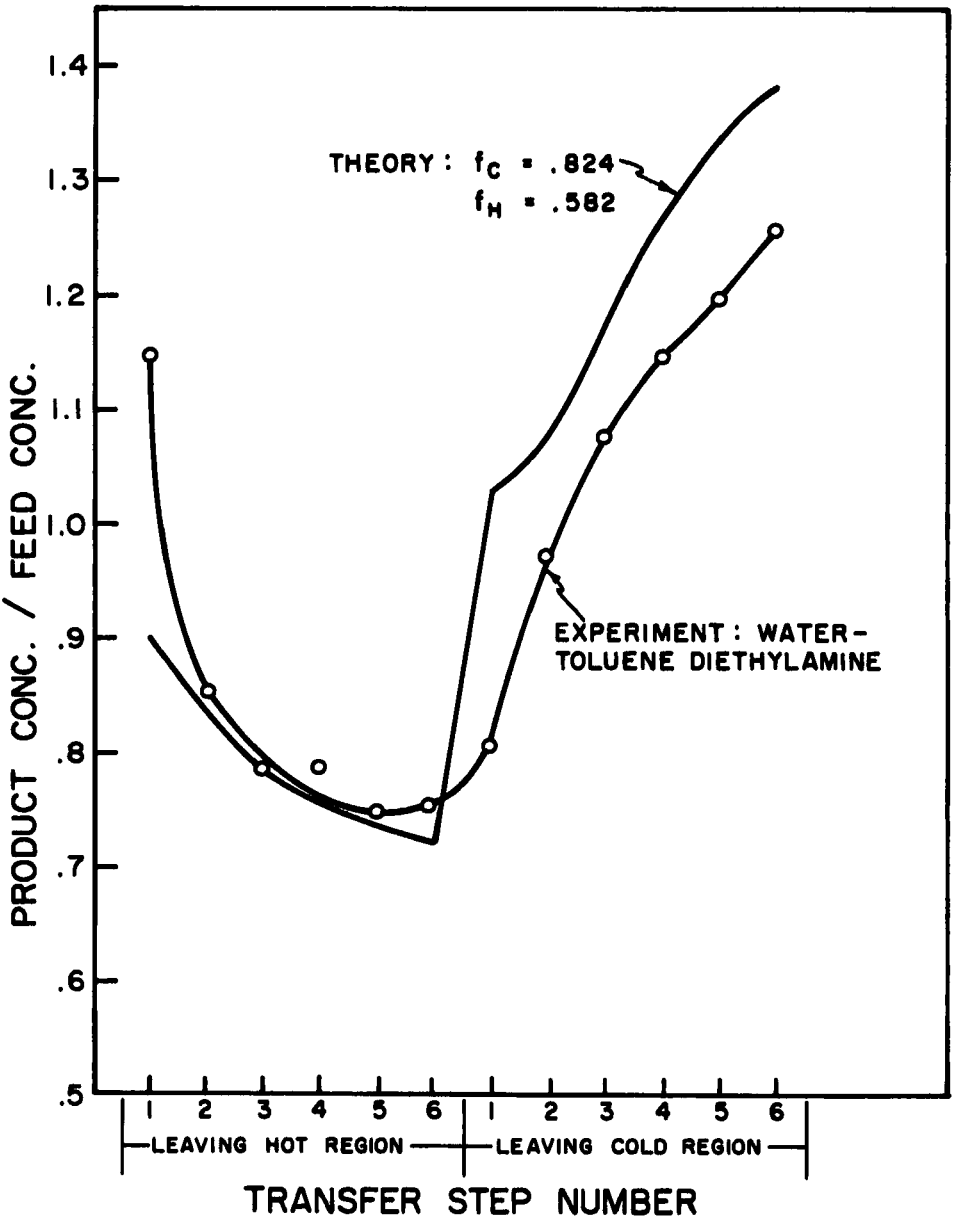

FIGURE 7

Comparison Between CCD Direct Mode Theory and Experiment for Diethylamine-Water Toluene System. 6 stages/region, 1 region, 6 transfers/half cycle.[6]

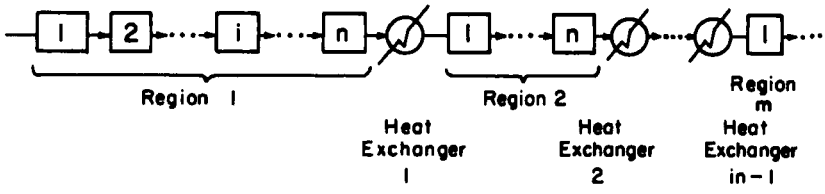

FIGURE 8

Staged Cycling Zone System for Traveling Wave Mode.[7]

heat exchanger between regions reforms the temperature wave and adjusts the temperature of the feed to region 2 to be 180° out of phase with the feed to region 1.

The periodic alternation of feed temperature causes a temperature wave in the system. The traveling temperature wave causes changes in the equilibrium distribution coefficient with the stationary phase rejecting solute when hot and storing solute when cold. As the solute moves from the moving phase to the stationary phase and back again, solute is concentrated in one part of the cycle and depleted in the other part resulting in a separation. Thermodynamic variables other than temperature can be used to change the equilibrium distribution of the solute and cause separation in the traveling wave mode. In particular, pH and ion strength have been used and will be discussed later.

The theoretical analysis of cycling zone separation in the traveling wave mode based on CCD theory follows the same lines as that for the direct mode systems. The variables S_H, S_C, V_M, c_M, c_S, $K_{i,j,s}$, $T_{i,j,s}$, $M_{i,j,s}$, and $f_{i,j,s}$ are defined the same here as for the direct mode case. In addition, several other variables are needed for the energy balances. C_{PM}, C_{PS}, and C_{PT} are the

heat capacities of the moving phase, the stationary phase, and the test tube, respectively. ρ_M, ρ_S, and W_T are the densities of the moving and stationary phase and the weight of the test tube, respectively. It is assumed that the densities and heat capacities are constant.

The fraction of solute in the moving phase of stage (i,j) after s transfers, $f_{i,j,s}$, is given by equation (1) of the previous section. The mass balances used to calculate the mass of solute in stage (i,j) after transfer step s are the same as those given for the direct mode in equations (2-4). The f values in equations (2-4) must be calculated using the temperature of each stage.

Assuming no heat loss from the separation system to the environment, the stage temperatures may be determined with energy balances. These energy balances for well insulated stages can be developed by defining A as the fraction of energy in the moving phase for any stage. By an analysis similar to that used to determine $f_{i,j,s}$, A can be found as:

$$A = \frac{C_{PM} V_M \rho_M}{(C_{PM} V_M \rho_M + C_{PS} V_S \rho_S + C_{PT} W_T)} \tag{7}$$

where, with the assumptions made here, A is independent of both temperature and concentration. The energy in stage (i,j) after transfer s equals the sum of the energy transfered from the previous stage in the moving phase and the energy left in the stage in both the stationary phase and the test tube. Using equation (7) to define A, this energy balance can be expressed in terms of temperature for $i \neq 1$ as

$$T_{i,j,s} = A\, T_{i-1,j,s-1} + (1 - A)\, T_{i,j,s-1} \tag{8}$$

If $i = 1$ but $j \neq 1$

$$T_{1,j,s} = A\, T_{HE,j-1,s} + (1 - A)\, T_{1,j,s-1} \tag{9}$$

If $i = 1$ and $j = 1$

$$T_{1,1,s} = A\, T_{FS} + (1 - A)\, T_{1,1,s-1} \tag{10}$$

where $T_{HE,j-1,s}$ is the temperature of material leaving heat exchanger j-1 for transfer step s, and T_{FS} is the temperature of

the feed for transfer step S. Because of the restrictive assumptions made previously, the energy balances in equations (8), (9), and (10) are independent of the mass balances and can be solved separately for any desired temperature, $T_{i,j,s}$. Using these temperatures, the f values can be calculated for each stage and transfer step, and then the mass balances may be solved.

The solution method for the traveling wave mode is analogous to the one used for the direct mode. A straight forward iterative solution can be obtained using equations (8-10) and (2-4) as recursion relations with the appropriate initial conditions. As indicated previously, a limiting repeating state solution can be obtained for a system of this type.[6,7]

Using an argument similar to the retention argument of chromatography,[10] the speed of both the concentration and thermal waves can be deduced. The average distance that solute will move is f x (number of transfer steps). By comparing the definition of f and A, equations (2) and (7), it is clear that A is a measure of the speed of the thermal wave. The distance the thermal wave travels is A x (number of transfer steps). Unless A = 1.0, the thermal wave will spread by the same band-spreading phenomena which spreads solute bands in chromatography and CCD. For low values of A, the thermal wave moves slowly and spreads out considerably giving very little separation. If A is near 1.0, the thermal waves will be sharp and will travel faster than the concentration waves. As the hot front of the thermal wave advances through a region, the fraction of solute in the moving phase increases sharply causing a concentration wave of high solute content to form behind the thermal wave. Behind the cold front of the thermal wave, a slow moving low concentration wave will form. Thus a considerable separation can be achieved by collecting separately the two concentration waves.

In order to study the validity of these theoretical predictions, the diethylamine-water-toluene system was studied in the traveling wave mode of cycling zone extraction. As in the

experimental study for the direct mode, water was the mobile phase, toluene was the stationary phase, and diethylamine was the solute that distributes between the two phases. The experimental apparatus consisted of test tubes held in a styrofoam insulating holder with a syringe for transfering the mobile phase. Several types of glass and plastic test tubes were used for stages since the type of test tube determined the value of A. In each experimental run, the system used had one region with 3 stages and with 4 transfers per half cycle. The distribution coefficient was curve fitted to account for both temperature and concentration dependence. More information on the experiment and the results is available in the original paper.[7]

For the traveling wave mode, the theoretical results are presented first in Figures 9-11 and the experimental results are compared with the theoretical predictions in Figure 12. The product temperatures and concentrations are shown in Figure 9 for a system with 1 region and 40 stages. The inlet temperature is a square wave, but the outlet temperature is no longer a square wave and is delayed behind the square wave. The outlet concentration wave is delayed behind the thermal wave with a maximum separation, α_{max} (= maximum concentration/minimum concentration) of 9.99. In comparison a system with 40 stages operated in the direct mode achieved separations of $\alpha_{max} = 1.78$ with 1 region and $\alpha_{max} = 6.62$ with 4 regions. The separation obtained for the traveling wave mode is clearly greater than what could be achieved in the direct mode. By increasing the number of stages for a single region traveling mode device to 160 stages, the separation can be increased to $\alpha_{max} = 108.9$.

The separation for a given system can be increased by optimizing the thermal wave velocity A. A can be varied to optimize the separation by changing the tube weight or heat capacity. In Figure 10, α_{max} is plotted versus the traveling wave velocity for a 40-stage system. There is an optimum value of 0.67 for A with $\alpha_{max} = 10.8$. Either high or low values of A are to be avoided since the separation is reduced significantly. The reason for

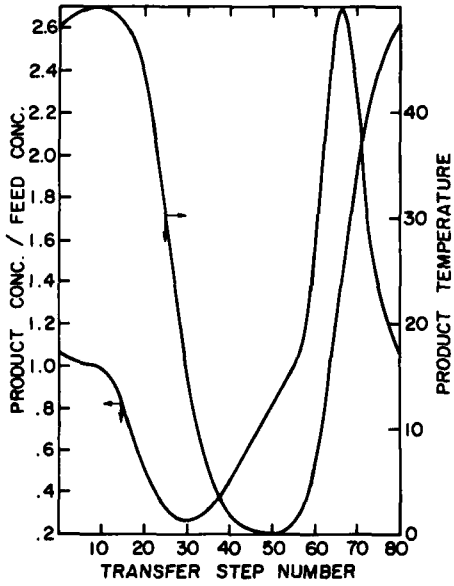

FIGURE 9

Product Concentrations and Temperatures for a Complete Traveling Wave Cycle: 40 stages/region, 1 region, $T_C = 0$, $T_H = 50$, $S_C = S_H = 40$, $K = 1.0 + 0.02T$, $A = 0.6$.[7]

poor separations at low values of A is evident from the temperature profiles in Figure 11. As the thermal wave velocity is decreased, the thermal wave becomes more diffuse and the temperature differences decrease. When this occurs, the variations of the distribution coefficient are minimized and there is less driving force for separation.

The reason for a separation maximum at an intermediate value of A, as shown in Figure 10, is quite complex. One would expect the separation to continue increasing as A approaches 1.0 since the thermal wave approaches a square wave with very sharp differences and correspondingly large differences in the distribution coefficient. However, the maximum separation actually occurs

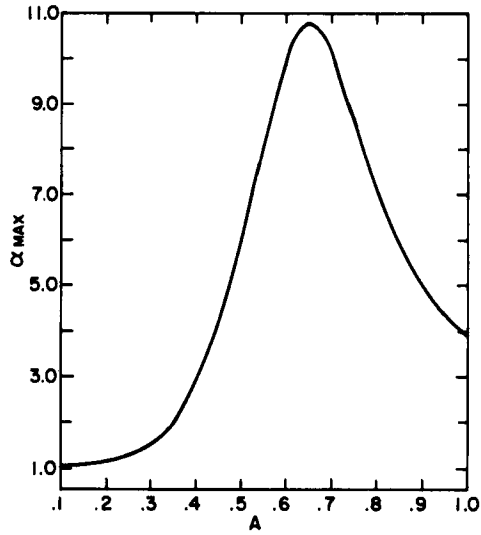

FIGURE 10

Effect of Thermal Wave Velocity, A, on Maximum Separation: 40 stages/region, 1 region, $T_C = 0$, $T_H = 50$, $S_C = S_H = 50$, $K = 1.0 + 0.02T$.[7]

when the thermal wave velocity is between the velocity of the two concentration wave velocities, $f_C < A < f_H$. An explanation of this will be delayed until the second model, the local equilibrium theory is discussed.

Theoretical calculations were also made to study the effects of variation of K values where smaller f values were used. Using an equation for K(T) of $K = 0.3333 + 0.003333T$, the resultant f values are $f_c = 0.25$ and $f_H = 0.333$. Although the ratio of f_c/f_h is unchanged from earlier cases, there is less separation at the optimum conditions. The optimum separation is obtained at $A = 0.3$ which is as expected since $f_c < A < f_h$. The separation at optimum conditions is about half as great for the case of lower f values. A similar result was obtained for the direct mode of operation.

For the direct mode of operation it was shown that increasing the number of regions increased the separation. Similarly, the

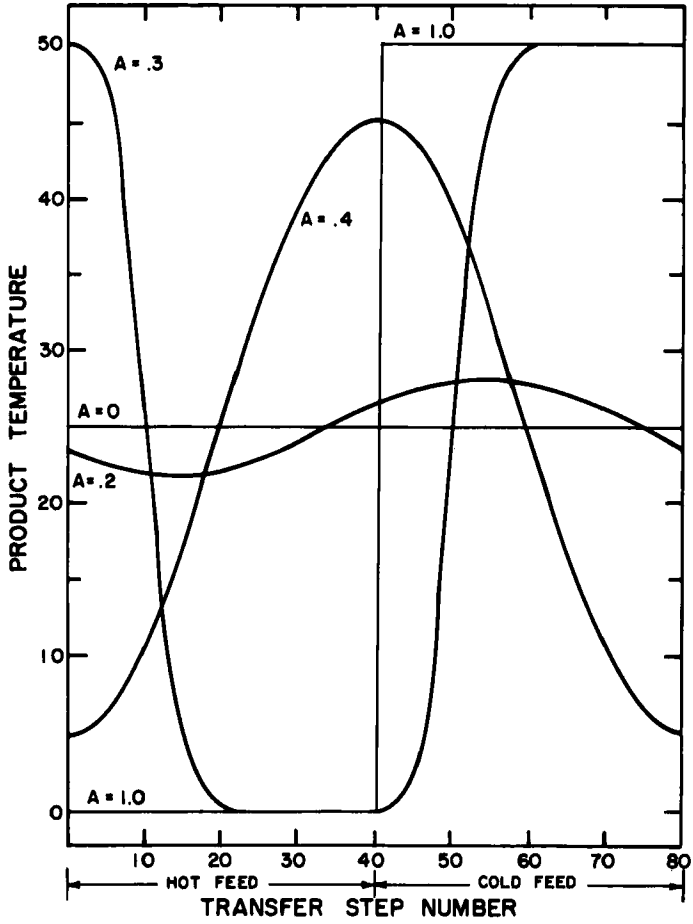

FIGURE 11

Product Temperature Profiles for Several Values of Thermal Wave Velocity: 40 stages/region, 1 region, $T_C = 0$, $T_H = 50$, $S_C = S_H = 40$, $K = 1.0 + 0.02T$.

traveling wave mode showed larger separations with more regions as well as an optimum number of transfers per half cycle. The optimum separation for this system with 4 regions and 10 stages per region was $\alpha_{max} = 20.9$. It is clear that the multiple regions

produce more separation, and that some optimum number of regions exist for a given number of stages.

The theoretical and experimental results are compared in Figure 12. This figure is for an all glass system where A = .466.

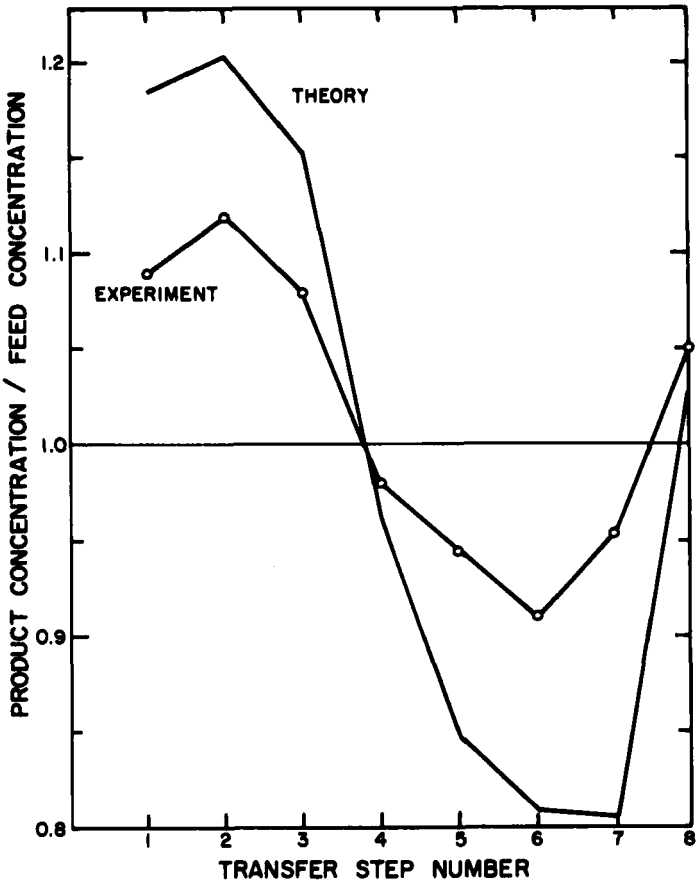

FIGURE 12

Comparison of Experimental and Theoretical results for an All-Glass System in Traveling Wave Mode. Experiment: diethylamine-water-toluene, $T_C = 0$, $T_H = 28$, 3 stages/region, 1 region, $S_C = S_H = 4$, Theory: $A = 0.466$, $K = 4.63 - 0.163T + 0.001707T.^2$

There is good qualitative agreement, but less separation was achieved than expected. The differences between experiment and theory might be expected since the theoretical model did not account for the concentration dependence of the distribution coefficient, the loss by evaporation, and the heat loss or gain of the system. However, this theory is quite useful in predicting the effect of changing variables and operating condition and optimizing the separation.

As indicated previously, thermodynamic variables other than temperature can be cycled to force a separation in the traveling wave mode of cycling zone extraction. It is well known that a change in ion concentration can change the distribution of a solute between two phases for certain systems. By varying the ion concentration of the feed to a cycling zone extractor, it should be possible to achieve a separation.

In order to illustrate the application of ion concentration to cycling zone separations, experiments were run to separate phenol red from water using 1-butanol as a stationary phase. These experimental results have not been presented previously. The concentration of sodium carbonate in the feed was used as the cyclic variable. This chemical system was chosen because the distribution coefficient changes significantly with ion concentration and the concentration of phenol red is easily determined with a spectrophotometer. The feed to a CCD apparatus was of constant phenol red composition but the $Na_2 CO_3$ concentration was varied as a square wave starting at 3.5N for half the cycle and then switching to .1N for the remainder of the cycle. At low ion concentration the stationary 1-butanol phase rejects solute, and at high ion concentration the solute is stored in the stationary phase.

The experimental results are shown in Figure 13. A good separation is achieved and the plot resembles those obtained for temperature cycling in the traveling wave mode. In Figure 13, a maximum separation of $\alpha_{max} = 39.0$ was obtained. For systems

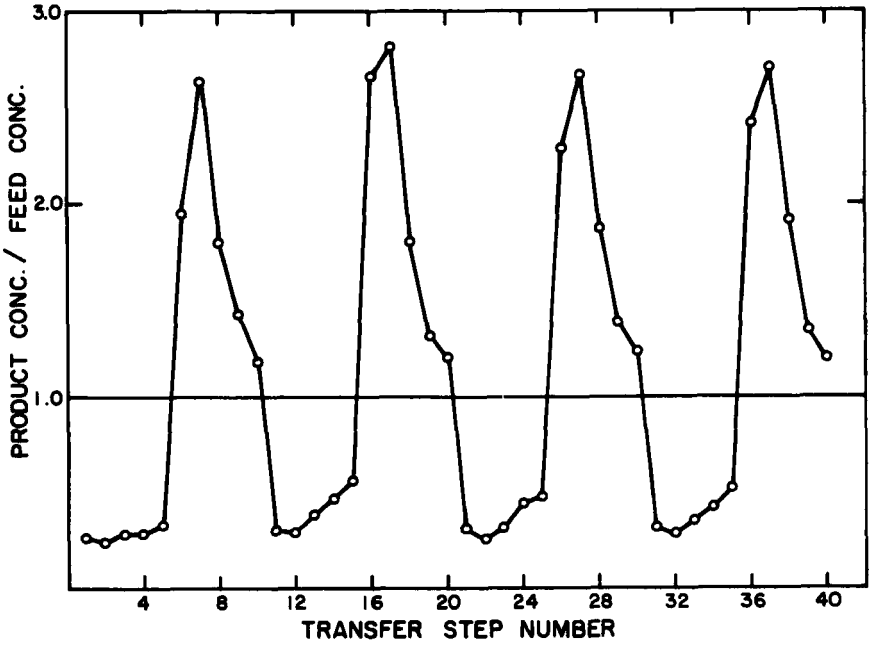

FIGURE 13

Product Concentrations vs. Transfer Step Number with Sodium Carbonate Concentration as the Cyclic Variable. Experiment: phenol red-water-1-butanol, 5 stages/region, 1 region, Low Na_2CO_3 concentration = 0.1N, High Na_2CO_3 concentration = 3.5N, 10 transfer steps per cycle.

where the distribution coefficient is significantly changed by ion strength, this technique could prove very useful.

Although the theory and results presented in this section are for discrete equilibrium staged systems, they are qualitatively applicable to continuous flow systems. If the number of theoretical plates for the continuous separation is relatively large, there is good agreement with this theory. The zone-broadening phenomena is well modeled by this system. In addition, the theory and results presented here are meant to establish a good intuitive feel for how the separation occurs and how it can be optimized.

LOCAL EQUILIBRIUM MODEL

Theoretical Development

Counter-current distribution, although a simple theory, was not the original theory used to explain cycling zone adsorption. Baker and Pigford[11] presented a local equilibrium model to theoretically explain their new separation process. This local equilibrium model for cycling zone adsorption was an outgrowth of a similar model for "parametric pumping" developed by Pigford, et. al.[12] and provided a means for evaluating fixed-bed experimental data. The following is a simplified discussion of the local equilibrium model.

Consider the process shown in Figure 14 in which a solute of concentration, c_o, flows through a fixed-bed of solid particles of length L. The temperature of the bed is periodically varied, either by heating and cooling the column walls as in Figure 14a (direct mode) or by using a heat exchanger to heat and cool the input stream as in Figure 14b (traveling wave mode). For both modes of operation, in this case, the temperature is cycled in a square wave of frequency $\omega/2\pi$ cycles/min. between a cold temperature, T_C, and a hot temperature, T_H. For column applications this represents the same system as Figures 1 or 8 discussed previously. The above can be summarized as a set of boundary conditions. For the traveling mode process, they are

$$c = c_o;\ z = 0,\ t > 0 \tag{11}$$

$$T = T_C + (T_H - T_C)\ sq\ (\omega t);\ z = 0,\ t > 0 \tag{12}$$

For the process described in Figure 14 Baker and Pigford presented four mass and energy balance equations. Two of the equations were solute and energy balances on the solid phase and two were solute and energy balances on both the fluid and solid phases. These latter two equations are shown below.

$$\underbrace{\frac{\partial c}{\partial t}}_{1} + \underbrace{\frac{(1-\alpha)\varepsilon}{\alpha}\frac{\partial c^*}{\partial t}}_{2} + \underbrace{\rho_s\frac{(1-\alpha)(1-\varepsilon)}{\alpha}\frac{\partial q}{\partial t}}_{3} + \underbrace{v\frac{\partial c}{\partial z}}_{4} - \underbrace{(E_D + D_M)\frac{\partial^2 c}{\partial z^2}}_{5} = 0 \tag{13}$$

$$\underbrace{\frac{\partial T}{\partial t}}_{1} + \underbrace{\left[\frac{\rho_s C_s (1-\varepsilon)}{\rho_f C_f \alpha} + \frac{\varepsilon}{\alpha}\right](1-\alpha)\frac{\partial T_s}{\partial t}}_{2} + \underbrace{v\frac{\partial T}{\partial z}}_{3} - \underbrace{(E_D + D_T)\frac{\partial^2 T}{\partial z^2}}_{4} = \underbrace{\frac{h_w q_w}{\rho_f C_f \alpha}(T_w - T)}_{5} \qquad (14)$$

The above equations disregard radial gradients in velocity, concentration, and temperature. The equations have been broken down into separate parts. For the mass balance equation (13), terms 1-3 represent accumlative contributions. The first term is the change in concentration with respect to time for the mobile phase. The second term is the change in concentration for immobile fluid trapped in the pores of the solid adsorbent, and the third term represents the change in concentration for the solid stationary phase. Terms 4 and 5 describe the mass transfer for an infinitesimal cross section of the packed column. The fourth term depicts convective mass transfer; that is, the common (input - output) contribution. Finally, the fifth term represents mass transfer due to dispersion and diffusion.

For the energy balance equation (14), terms 1 and 2 represent accumulative contributions. The first term is the change in temperature of the mobile phase with respect to time. The second term describes temperature changes with respect to time for the stationary phase which includes the solid adsorbent and trapped immobile fluid. The third term expresses the rate of temperature change with respect to axial distance, z, due to convection and the fourth term expresses the rate of temperature change as a result of dispersion and diffusion. Finally, the fifth term represents the amount of energy in terms of heat that is transferred from the surroundings to the column.

Following Baker and Pigford[11] these equations can be simplified by applying several assumptions. If mass and energy

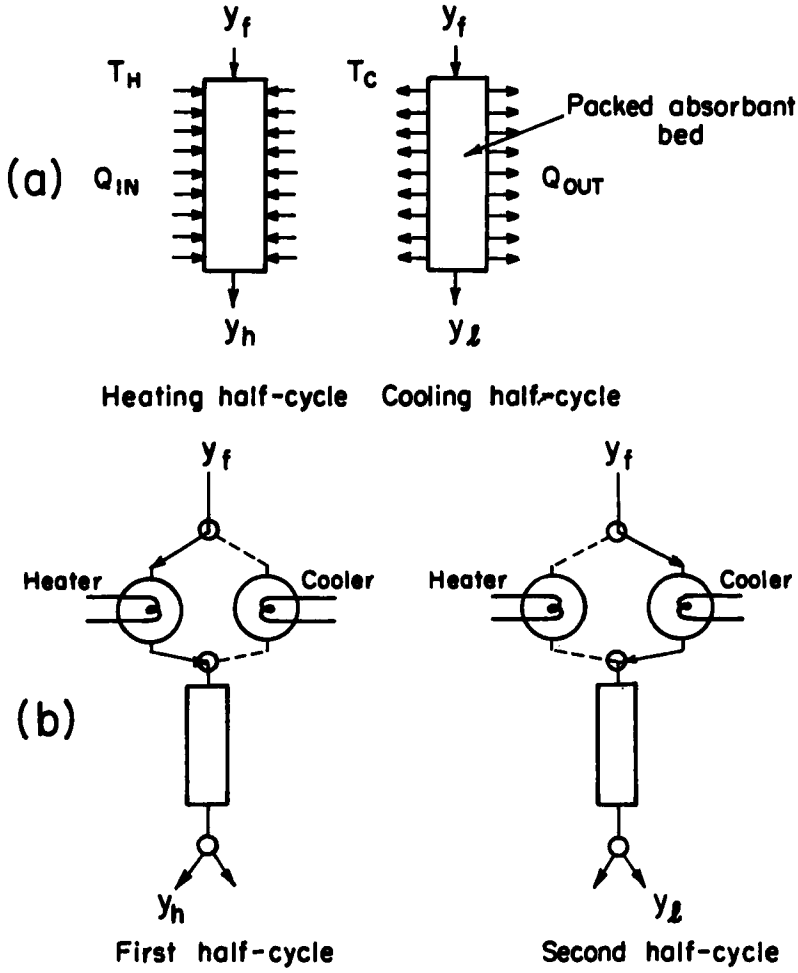

FIGURE 14

Single-Zone Operation of Cycling Zone Absorber. The Direct Wave Mode is Indicated by (a) above; (b) below. Illustrates the Traveling Wave Mode.

transfer rates are assumed to be very high, then not only is the immobilized fluid in the pores in local equilibrium with the adsorbent but all fluid and solid phases are in equilibrium (i.e., $c = c^*$, $T_s = T$). Secondly, the solid phase concentration is assumed to be a function of temperature and concentration only and heat capacities and densities are assumed to be independent of temperature and concentration.

$$q = f(T,c) = f(T_s,c^*) \tag{15}$$

Finally, the dispersive and diffusive terms are neglected and the simplified equations for linear isotherms ($q = A\,c^*$) result.

$$\frac{\partial c}{\partial t} + \mu_c \frac{\partial c}{\partial z} = \frac{-\mu_c}{v} \frac{1-\alpha}{\alpha} (1-\varepsilon)\,\rho_s \frac{\partial q}{\partial T} \frac{\partial T}{\partial t} \tag{16}$$

$$\frac{\partial T}{\partial t} + \mu_{th} \frac{\partial T}{\partial z} = 0 \tag{17}$$

where

$$\mu_c = \frac{v}{1 + \frac{1-\alpha}{\alpha}\,\varepsilon + \frac{1-\alpha}{\alpha}\,(1-\varepsilon)\,\rho_s A} \tag{18}$$

$$\mu_{th} = \frac{v}{1 + (1-\alpha)\,[\rho_s C_s (1-\varepsilon) + \rho_f C_f \varepsilon]/\rho_f C_f \alpha} \tag{19}$$

A = constant of proportionality for the linear isotherm and is a function of temperature only.

As shown previously, temperature and concentration move through a packed column in waves; in this case, the concentration wave velocity is given by μ_c and the thermal wave velocity is given by μ_{th}. These wave velocities are adjustable and depend on values for the parameters in the denominator of each equation.

Using the boundary conditions given for the process in Figure 14b the solution to equation (17) is

$$\frac{dz}{dt} = \mu_{th} \tag{20}$$

Note that equation (20) is a total derivative since the temperature dependence has been eliminated. The solution is shown in Figure 15 for the traveling wave process. For the direct mode

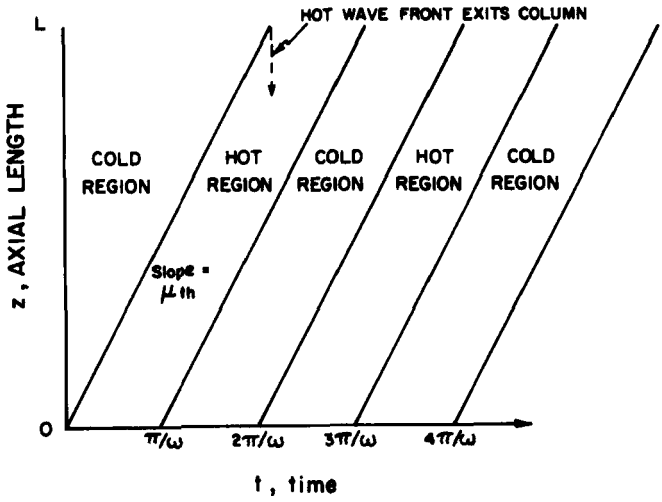

FIGURE 15

The Solution of the Energy Balance Equation.[3]

process (Figure 14a), $\mu_{th} \to \infty$ and the lines shown on Figure 15 would then be vertical. Note that at any particular time, the column can contain several thermal regions. The number of thermal regions possible increases with column length and cycling frequency, and decreases with higher values of μ_{th}. Along the lines of slope, μ_{th}, temperature is constant.

Baker and Pigford solved the solute mass balance, equation (20) by using the same boundary conditions as above and a technique known as the method of characteristics. The solution can be expressed as

$$\frac{dz}{dt} = \mu_c \tag{21}$$

and Figure (16a) shows the solution plotted for the traveling wave process. The solution yields lines in the figure called characteristics. As a result of the method used to solve equation (16), the concentration, c, along these characteristics

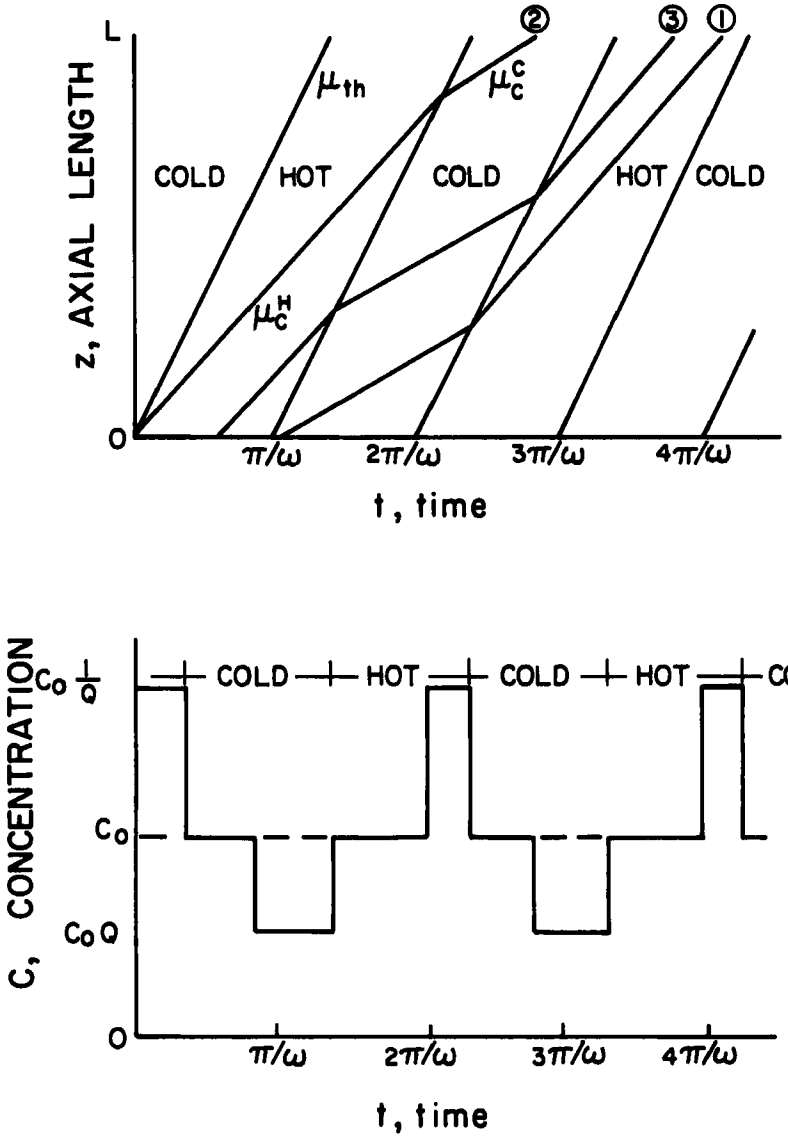

FIGURE 16

(a) above, Solution of Mass Balance Equation; (b) below, Effluent vs. Time for System Represented by (a).

must remain constant. In a general sense, these characteristic lines can also be thought of as the path of an average solute molecule moving through the column at a velocity, μ_c. An intuitive feel for this solution can be obtained by noting that if $\frac{\partial T}{\partial t} = 0$, equation (16) reduces to a form analagous to the energy balance equation, and thus should have a similar solution. Indeed, within a thermal region $\frac{\partial T}{\partial t} = 0$ and equation (20) and (21) are quite similar. Figure 16a shows that μ_c has different values depending on the temperature of the region. Adopting the convention that solute is stored by the solid phase at low temperature and released at high temperatures, the value of (A) in equation (18) will be low when $T = T_H$ and high when $T = T_C$. Equation (18) shows that this, indeed, leads to different μ_c values and $\mu_c^H > \mu_c^C$.

When a characteristic passes from a warm region into a cold one, or vice versa, the thermal wave causes a discontinuity to exist at the boundary. At this wave front the total mass does not change; however, the mass is redistributed. For a linear isotherm Baker and Pigford derived the following equation for this redistribution:

$$\frac{c_C}{c_H} = \frac{\frac{1}{\mu_c^H} - \frac{1}{\mu_{th}}}{\frac{1}{\mu_c^C} - \frac{1}{\mu_{th}}} = Q < 1 \qquad (22)$$

The concentration of solute molecules changes by a factor Q when passing from a warm region to a cold region. Likewise, the concentration changes by a factor 1/Q when passing from a cold region to a warm region. Intuitively, this phenomenon is not difficult to understand. As cold solute molecules of concentration, c_C, are overtaken by a hot thermal wave, the stationary phase releases solute and the concentration instantaneously increases to c_H. When warm solute molecules, c_H, are overtaken by a cold thermal wave, the stationary phase stores more solute and the concentration instantaneoulsy decreases to c_C.

Figure 16b shows the exit concentration of solute versus time based on the values of μ_{th}, μ_c^C, and μ_c^H represented on Figure 16a for the process discussed in Figure 14b. The areas where the solute concentration is c_o/Q represent exiting solute molecules which have been overtaken by only one hot thermal wave. (Line 1). The areas where the solute concentration is c_oQ represent exiting solute molecules which have been overtaken by only one cold thermal wave (Line 2). In the case of areas where the effluent concentration is c_o, these solute molecules were overtaken by two or a multiple of two thermal waves since $c_o(Q)(1/Q) = c_o$ (Line 3). This is similar to the interference reported in connection with Figures 3 and 5 discussed earlier.

It is now clear that the cycling frequency of thermal waves is important. Ideally, no solute molecule should be overtaken by two thermal waves for maximum separations. Indeed, Baker and Pigford showed that this criterion provided the optimum separation factor for a one zone system.

In addition to thermal wave frequency, another method exists for maximizing separation. Suppose a thermal wave can be made to pass through the bed at any velocity desired, overriding the natural wave. An example would be to move a heat source along the column at some arbitrary velocity, μ_{th}, as done by Zhukhovitiskii.[13] Suppose further that $\mu_c^H > \mu_{th} > \mu_c^C$. For this case, the separation factor, α_{av}, tends toward infinity. However, equation (22) will not be strictly applicable now. With $\mu_c^H > \mu_{th}$, equation (22) gives negative values of Q since $\frac{1}{\mu_c^H} - \frac{1}{\mu_{th}}$ is now less than zero. Thus, to explain the reason for an infinite separation, reference will be made to Figure 17. As a concentration wave of velocity μ_c^C moves through the column, a hot thermal wave will eventually overtake it if the column is long enough. At this point the concentration wave is trapped. If the solute speeds up to μ_c^H, it finds itself immediately in a cold region and must slow to μ_c^C and be overtaken by the same hot thermal wave. Likewise, a concentration wave of velocity μ_c^H will

eventually overtake the leading edge of a similar hot thermal wave and also become trapped. Thus, as Figure 17 shows, essentially all the solute is forced to exit the column with the leading edge of the hot thermal wave and little or no solute exits with the leading edge of the cold thermal wave. The separation factor is essentially infinite. This is the potential power of cycling zone adsorption in the traveling wave mode. Note that the above discussion pertains only to conditions where $\mu_c^H > \mu_{th} > \mu_c^C$.

As explained earlier in the direct mode of operation the thermal wave velocity, μ_{th}, is essentially infinite. The theoretical development presented in Figures 15 and 16 is equally applicable to the direct mode except that the thermal wave fronts are vertical instead of slanted. The definition of Q found in equation (22) is the same for the direct mode as the traveling

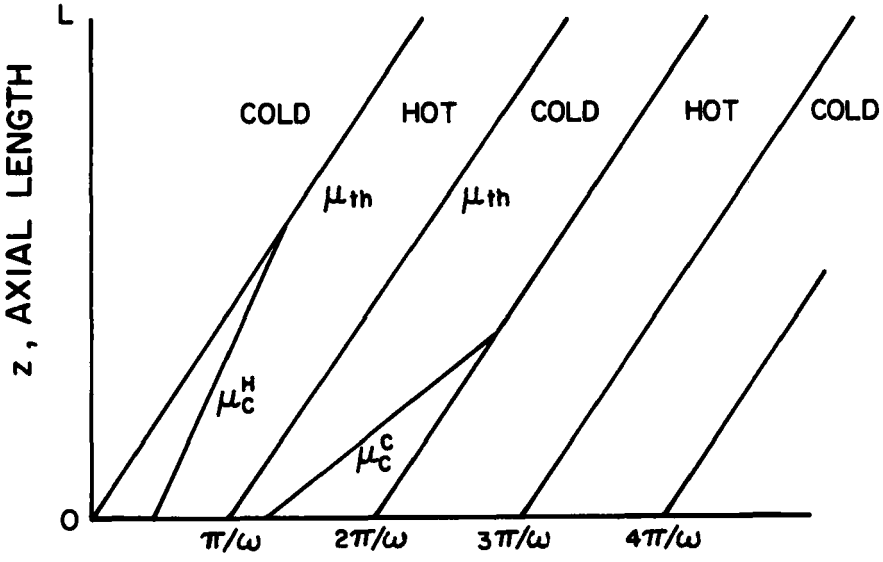

FIGURE 17

Characteristic Lines Showing case of Infinite Separation.

wave mode. However, separations using the direct mode are inherently not as good as those obtained in the traveling wave mode. Since $\mu_{th} \to \infty$, μ_c^H can never be greater than μ_{th} and infinite separations of the kind discussed in regard to Figure 17 are not possible. Also, reference to equation (22) shows that, with μ_c^H and μ_c^C held constant, the highest value of Q and thus the poorest separation is obtained when $\mu_{th} \to \infty$ as in the direct mode.

This, then, is the basis of the local equilibrium model. Starting with mass and energy balances, a theoretical prediction has been obtained for the exit solute concentration from a packed column. With the assumptions used and the stipulation of linear isotherms, this model, as presented, is highly idealized. However, by expanding the theory to systems of columns in series and by using non-linear isotherms such as the Freudlich isotherm ($q = A(c^*)^k$). This theory models the real world qualitatively.

EXPERIMENTAL SUPPORT OF LOCAL EQUILIBRIUM MODEL

Baker and Pigford[11] studied the separation of acetic acid from water on activated carbon to demonstrate the feasibility of cycling zone adsorption and of the local equilibrium theoretical model. Figure 18 shows their results for a single zone in the direct (standing wave) thermal mode. This process arrangement is similar to the one shown in Figure 14a previously. In Figure 18, non-linear Freudlich isotherms were used in the local equilibrium model to predict the effluent concentration. Note that even with the non-linear isotherms, the theoretical results are similar to those of Figure 16b. Hot and cold half-cycles were approximately 1000-1200 sec. long. In the figure the data for the cold half-cycle has been shifted one half cycle forward. If the experimental data had been plotted chronologically, the cold half-cycle would have begun at about 1100 sec. instead of zero time. The theoretical high and low concentrations follow the

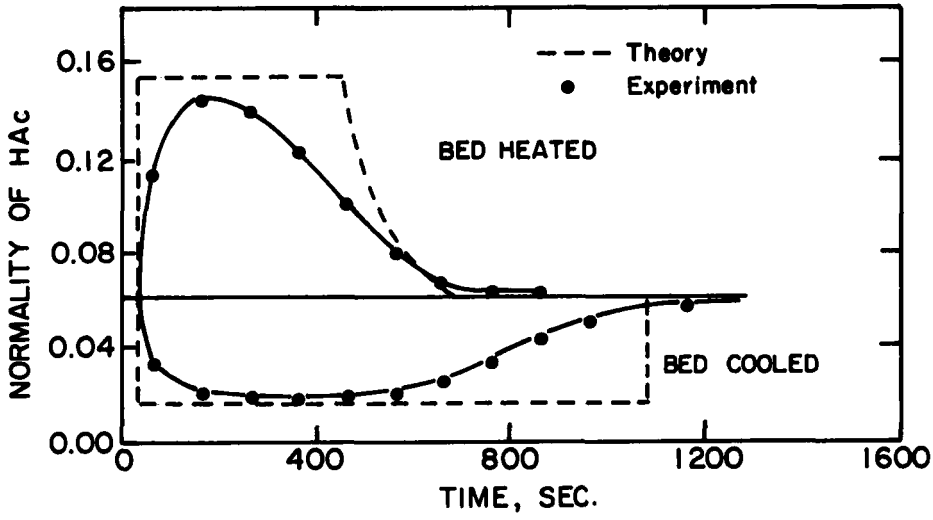

FIGURE 18

Effluent Concentration Profile for a Singel Zone System in the Direct Wave Mode: T_C = 3.5°C, T_H = 58.9°C, Acetic Acid Feed Concentration = 0.0611ON, Frequency = 0.03 cycles/min, Activated Carbon Adsorbent.

expected c_o (1/Q) and c_oQ values if $Q \gtrsim 0.4$ for the process since $\mu_{th} \to \infty$ and $\mu_{th} >> \mu_c^H$. The experimental results are in good qualitative agreement with theory; however, the effect of neglecting dispersion terms in the local equilibrium model is evident in the rounded experimental peaks.

Figure 19 shows experimental results comparing the direct and traveling wave mode. Again, the system involves the separation of acetic acid from water and both modes used a single-zone process similar to Figures 14a and 14b. The theoretical and experimental results illustrate the inherent superiority of the traveling wave mode over the direct mode as noted earlier. As in the previous figure, the data for the cold half-cycle has been shifted by one half cycle. At the end of each half-cycle the effluent concentration is seen to approach c_o for both modes of operation. As

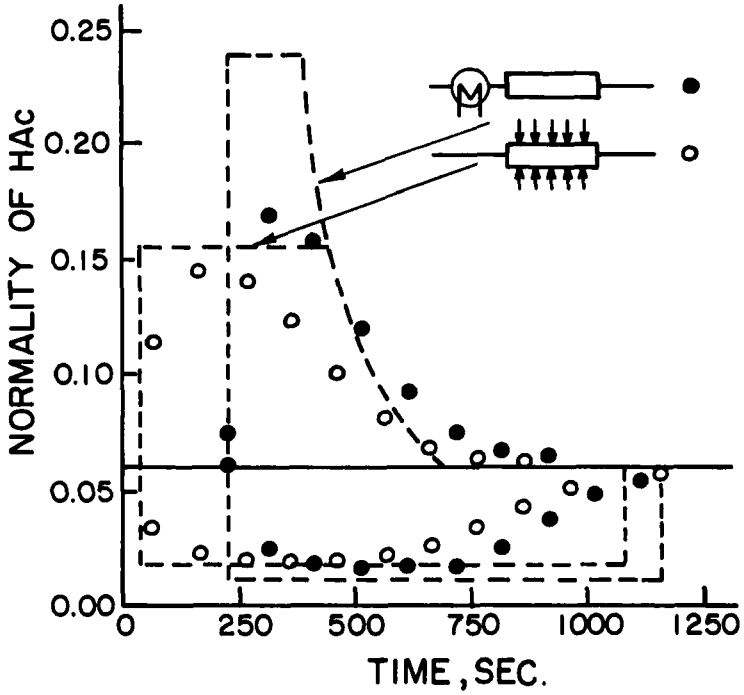

FIGURE 19

Comparison of Direct and Traveling Wave Modes for a Singel Zone System: T_C = 3.5°C, T_H = 58.9°C, Acetic Acid Feed Concentration = 0.0610N, Frequency = 0.03 Cycles/min., Activated Carbon Adsorbent.[11]

explained in the theoretical development and in the CCD section, this is caused by solute molecules being overtaken by more than one thermal wave before exiting the column. To alleviate these regions of no separation or "shoulders", shorter cycle times could be used.

Other models and theories have been advanced to explain the mechanism of cycling zone adsorption. Gupta and Sweed[14] and Meir and Lavie[15] have proposed more mathematical models utilizing the concepts of local equilibrium. However, Baker and Pigford's model was presented above because of its relative simplicity and lack of extensive numerical calculations.

COLUMN APPLICATIONS OF CYCLING ZONE ADSORPTION

Many researchers, besides Baker and Pigford, have utilized the cycling zone adsorption technique to experimentally investigate existing commercial separations. The experimental work of Van der Vlist,[16] Busbice and Wankat,[9], and Ginde and Chu[17] are representative of the varied possible applications of cycling zone adsorption and two of these are amenable to comparison with the local equilibrium model.

Van der Vlist[16] studied the separation of oxygen and nitrogen from air using a molecular sieve adsorbent. The adsorbent preferentially retained nitrogen at low temperatures and desorbed nitrogen at higher temperatures. Thus, gas exiting a cold region had a higher concentration of oxygen and gas leaving a hot region had a relatively lower concentration of oxygen. A two zone direct mode system was used. The temperatures of the two fixed-bed columns were cycled as sine waves and the temperature of each zone was 180° out of phase with that of the other. Figure 20 shows the experimental results for this two zone system. A maximum separation factor for oxygen of 10.6 was achieved. Observe that the shape of oxygen concentration curve resembles that obtained by Baker and Pigford in Figure 18 for their separation of acetic acid and water. Van der Vlist's research points out one potential problem with separations involving high solute concentrations and gaseous components. The alternate adsorption and desorption of solute and expansion and contraction of gas due to temperature cycling cause large flow fluctuations in product streams. Van der Vlist used two columns in series to partially minimize this effect.

In the cases studied thus far in connection with the local equilibrium model, temperature has been used as the cyclic variable to force separation. However, reference to equations (13) - (17) and earlier discussion show that any thermodynamic variable can be used in the traveling wave mode as long as the following criteria are satisfied; (1) the solid phase concentration

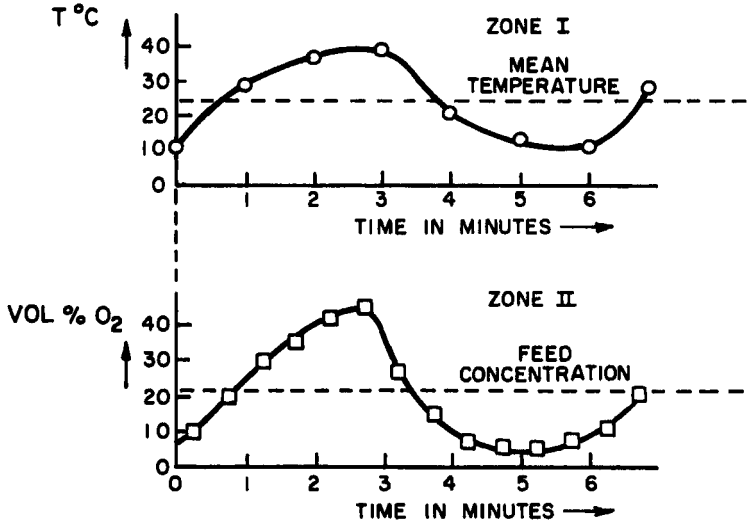

FIGURE 20

Temperature and Oxygen Concentration as a Function of Time for Nitrogen-Oxygen Concentration as a Function of Time for Nitrogen-Oxygen Separation: T_C = 10.2°C, T_H = 38.7°C, Frequency = 0.167 cycles/min., 45-50 mesh Linde Molecular Sieve Type 5 A Adsorbent.[11]

must be a function of this variable, and (2) the velocity of the variable wave must be known or measurable. Busbice and Wankat[9] and Busbice[18] utilized pH as the cyclic variable to remove fructose and glucose from water. Using a dihydroxborylphenyl-succinamyl derivative of aminoethyl cellulose (DBAE cellulose) as an adsorbent in a fixed-bed column, pH waves were sent through the column in a cyclic square wave pattern varying from a low pH of 5.0 to a high pH of 8.5. For the sugar separations studied, adsorption was high at basic pH and almost negligible under acid conditions. Thus, retention was an approximately on-off mechanism. In regions of the column where pH was low, the mobile phase was more concentrated in fructose and glucose. In regions where pH was high, the mobile phase was depleted of its fructose and glucose.

In the discussion of the local equilibrium model a condition for maximizing separations was presented. In terms of pH as the cyclic variable, this condition can be rewritten as

$$\mu_c^{\text{low pH}} > \mu_{pH} > \mu_c^{\text{high pH}} \tag{23}$$

For the separations investigated by Busbice,[18] this condition was satisfied. Reference to Figure 21 shows a fructose separation from Busbice's experimental work. A peak-to-peak separation of approximately 4.0 was obtained. Although the separation factor was certainly not infinity, the figure shows that most of the fructose exited with the leading edge of the low pH wave and little fructose exited with the high pH wave. For this experimental plot the cycles were 4.4 column volumes long and there is little indication of the "shoulders" prevalent in Baker and Pigford's data. This indicates that the exiting solute molecules were overtaken by only one thermal wave or an odd number of thermal waves. The experimental data also shows that with periodic variations in the thermodynamic variable, the exiting solute concentration is also periodic. Figure 21 shows that a repeating state is reached.

A separation of both glucose and fructose from water appears in Figure 22. This figure illustrates that the two sugars compete for the active sites on the cellulose packing; the conformation of fructose being more desirable than that of glucose. As a result, the separation factor for fructose of 3.5 is not quite as good as that for fructose alone. In Figure 22 the so called "shoulders" are very pronounced due to the long cycles of 7.8 column volumes. This indicates that some of the exiting solute molecules were overtaken by two thermal waves or a multiple of two thermal waves. Shorter cycle times would correct this situation and improve the average separation as Figure 21 indicated. With regard to potential multi-component separations, it is important to observe that this figure shows no tendency for the separation of glucose from fructose; both sugars exit the column

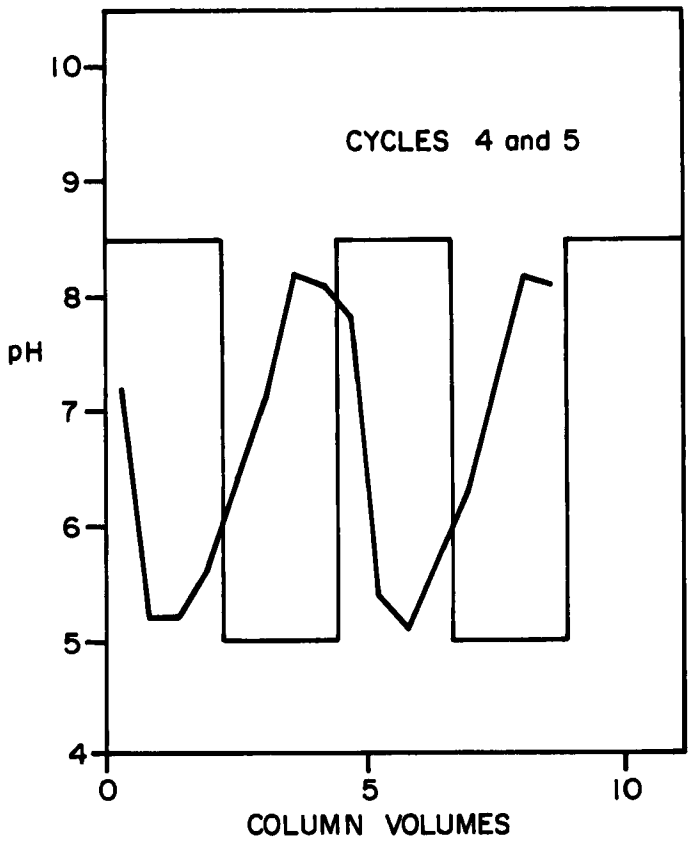

FIGURE 21a

Cycling Zone Separtion Using Fructose in Water. a) shows the pH waves.

at the same time. However, subsequent discussion on multi-component separations will show that this is an expected result for the traveling wave patterns discussed until now. The sugar separations results presented here have not been previously presented in the open literature.

All the experimental work, thus far, has used only one mode of operation, either the direct mode or the traveling mode. One

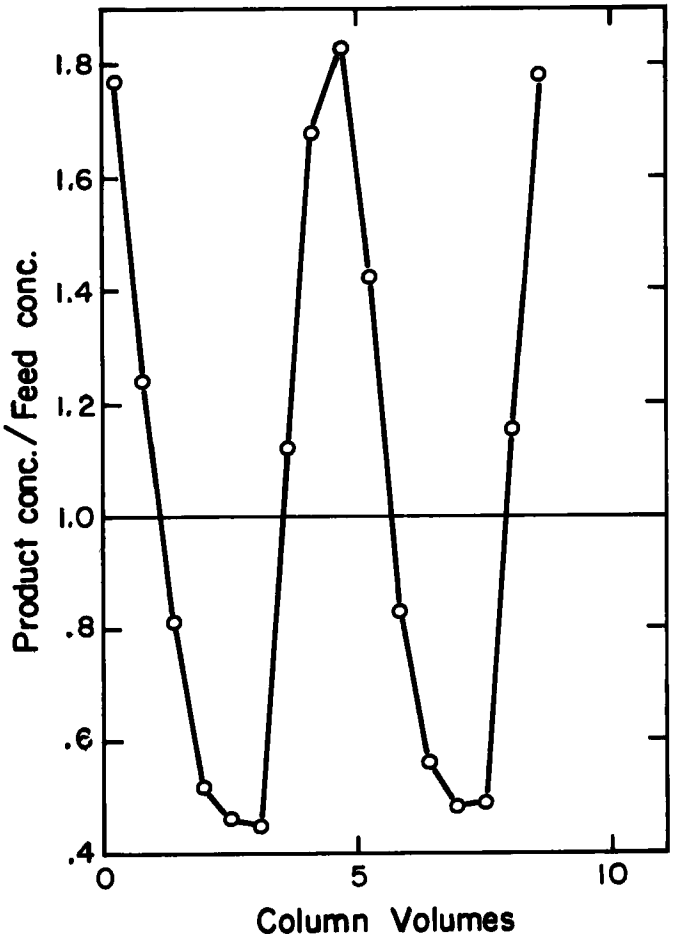

FIGURE 21b

Cycling Zone Separation Using Fructose in Water. b) shows the coutlet concentration for Cycles 4 and 5: 4.4 Column Volumes/cycle, Flow rate = 0.76 ml/min, Feed Concentration = 4.0 mg/ml, Temperature = 25°C[8] Morpholine and Acetic Acid are used as Buffers for pH waves.

might wonder if a combination of modes would be advantageous or feasible. Busbice and Wankat[9] investigated the use of a

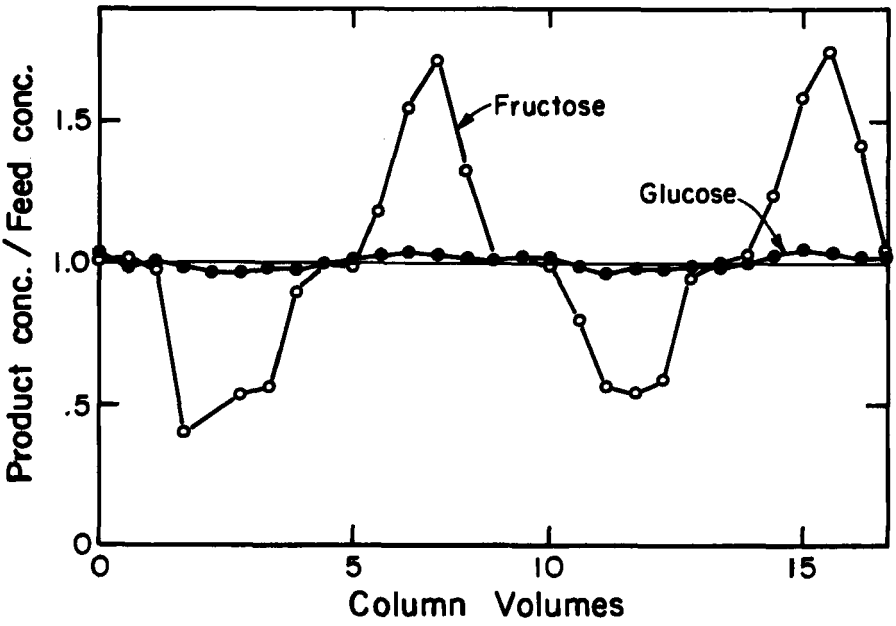

FIGURE 22

Cycling Zone Separation of Glucose and Fructose Showing Outlet Concentration Waves: 7.8 Column Volumes/cycle, Feed Concentration = 4 mg/ml, Temperature = 25°C, Flow rate = 0.76 ml/min, 0.6 g. DBAE Cellulose Adsorbent.[18]

simultaneous pH traveling wave and temperature direct mode in the separation involving fructose and glucose. In addition, Ginde and Chu[17] used a combined thermal direct and traveling wave mode to separate NaCl from water. The experimental apparatus consisted of two columns filled with mixed ion exchange resins and two well-mixed hot and cold reservoirs. Salt solutions were enriched when leaving a bed of hot resin and depleted when leaving a bed of cold resin. Operation entailed simultaneous flow of hot NaCl solution through a cold column to the cold reservoir. After a specified half cycle time, flow from the hot reservoir was diverted to the previously cold resin bed and flow from the cold reservoir was

diverted to the previously hot resin bed. Cycles were performed in this manner and the separation factor reported. The resin beds were heated by the walls of the column and cooled by the passage of cold salt solution. Thus, desorption in a hot bed was in the direct mode and adsorption in a cold bed was in the traveling wave mode. Ginde and Chu obtained maximum separation factors of 1.387 for this system using 0.05 M brine solutions.

MULTI-COMPONENT CYCLING ZONE SEPARATION

An area of cyclic separations which has received little attention until recently is multi-component separations. In the past, experimental and theoretical work was concerned only with removing all solutes together from the feed. Wankat[8] has extended the local equilibrium model and the equilibrium stage model for single components to a method of separating multi-component mixtures using the traveling wave mode. As of yet, no experimental results have been presented in the literature. This aspect of the cycling zone technique may prove to be the most useful in the future.

Both of the cycling zone models predict that solutes can be recovered individually if the cyclic variable is input into the column in a series of steps (see Figure 23) instead of as a square wave. For each chemical system, the step sizes must be chosen so that some components will move faster than the wave velocity and some slower. By having appropriate step sizes, a multi-component separation may be obtained with each component concentrating at that step where its wave velocity first becomes faster than the velocity of the cyclic variable.

As an example, consider the separation of two components, A and B, by adsorption from a non-adsorbed carrier with temperature as the cyclic varible. Assume component A is more strongly absorbed than B at all temperatures and that both are less strongly absorbed as temperature increases. The feed to the column is as shown in Figure 23 with temperatures T_C, T_1, and T_2 input in that order. At the coldest temperature, T_C, both A

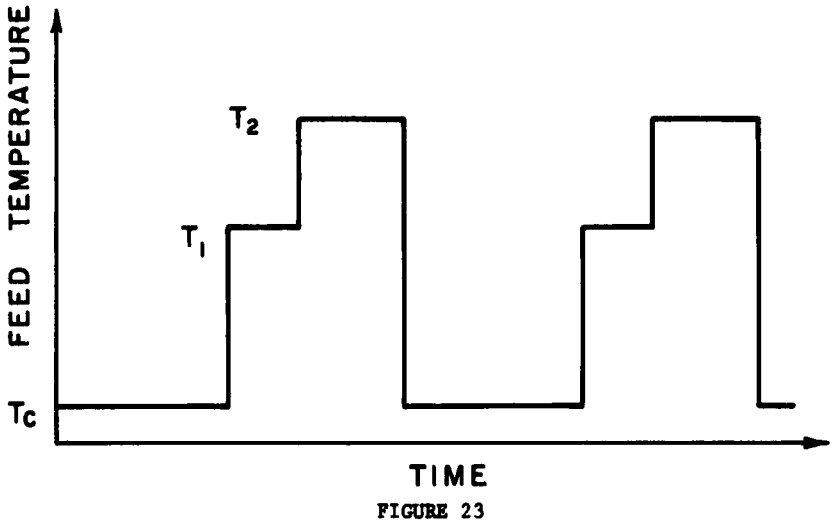

FIGURE 23

Feed Temperature Profile for Two Solutes in Multi-component Separation.[8]

and B move slower than the temperature wave and begin to fall behind the T_C wave until they are in the T_1 region of the wave. The temperature T_1 is chosen so that A now moves faster than the thermal wave and B moves slower. As a result, component B falls behind into the T_2 part of the wave and component A stays at the T_1 wave front. Component A will tend to be "trapped" at the T_1 wave front since the thermal wave overtakes all A at T_C and is overtaken by all A at T_1. The temperature T_2 is chosen so that both components move faster than the thermal wave. Component B will now concentrate at the T_2 wave front while component A moves past this thermal wave to the T_1 wave front. If the column is long enough and the times for each temperature are set properly, very large separations should occur. This argument is like that presented in the local equilibrium traveling wave mode section.

If more than two components are present, the feed can still be separated if additional temperature plateaus are added. A

separation can also be obtained by using a continuous change in the feed temperature between T_C and T_2 (either linear or non-linear). In this case, each component will tend to concentrate at the temperature where it moves at the same velocity as the thermal wave. Other cyclic variables may be used instead of temperature to obtain the same separation.

The local equilibrium theory of Baker and Pigford[11] can be easily modified to predict multi-component separations using an inlet temperature profile as shown in Figure 23. This has been done by Wankat[8] with the simplifying assumptions of local equilibrium and linear adsorption isotherms. In addition, axial dispersion, heat of adsorption, and solute-solute interactions are neglected. These are reasonable assumptions for a system with low solute concentrations and relatively small separations. This simplified model predicts that all of component A will exit at a point in time and all of component B will exit at a different point (infinite separation). There is no A or B in the rest of the cycle. In practice the infinite separation will not occur because of dispersion effects and non-linear isotherms.

To obtain a more realistic model which accounts for dispersion, the equilibrium stage model can be extended to multi-component cycling zone separation. Although the CCD-model is only approximate for continuous separations, it is relatively accurate when there are a large number of stages and transfer steps per cycle. Using the same assumptions stated previously for CCD models, very large separations can be achieved. An example of results of this model is shown in Figure 24 for a system of three solutes in a nonadsorbed carrier. The separation here is good but certainly not infinite. The overlap of peaks due to dispersion of the thermal wave is a major limiting factor on the separation. It is anticipated that this system could be further optimized to increase the separation.

There are some important restrictions which must be met if a multi-component system is to be separated by this technique. The

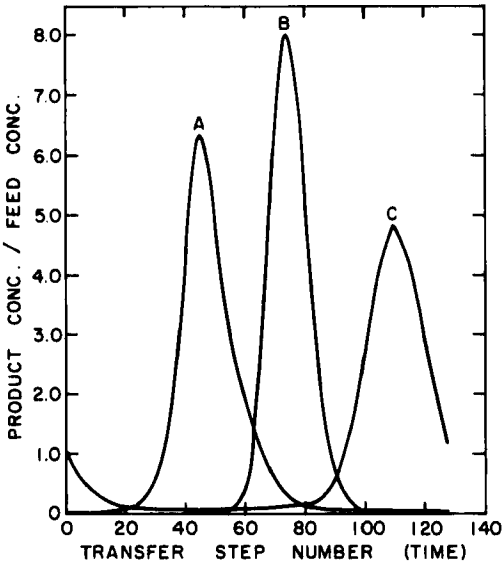

FIGURE 24

Results of stages Theory Calculation for Separation of Three Solutes. 160 stages, $T_c = 0$, $T_1 = 100$, $T_2 = 250$, $T_3 = 400$, $S_c = 40$, $S_1 = 32$, $K_c = 0.3333 + 0.00333T$.[8]

concentration wave velocities of each component must be different and must vary appropriately with the cyclic variable. In addition, a series of stringent restrictions which will produce a good separation are elucidated by Wankat.[8] All portions of the cycle must last a long enough period of time so that the thermal waves are reasonably developed. The sum of $T_C + T_2$ must be large enough to prevent the trailing edge of the slower moving component B from overlapping with the leading edge of the faster moving component A. Also, temperature T_1 must be large enough to prevent the trailing edge of the faster moving component A from overlapping the leading edge of the slower moving component B. There are also several less intuitive restrictions. The more

components in the system the more restrictions present. Any method which allows these restrictions to be satisfied will improve both the maximum purification and resolution of the components.

These theories show the feasibility of multi-component separations by the cycling zone technique. As the number of components increases the restrictions become more stringent, but theoretically any number of components can be separated as long as their distribution coefficients are different from each other and are temperature dependent. The predictions presented here are also valid for systems using cyclic variables other than temperature.

ACKNOWLEDGEMENT

The experimental assistance of Scott Jensen in preparation of Figure 13 is gratefully acknowledged. Permission to reproduce Figures 8, 9, 10, 11, 12 from Journal of Chromatography; Figures 14, 18, 19, 23, 24 from Industrial and Engineering Chemistry Fundamentals; and Figures 1, 2, 3, 4, 5, 6, 7, 20 from Separation Science is gratefully acknowledged. This work was partially supported by NSF Grant No. GK-43282.

REFERENCES

1. C.W. Skarstron, Ann. N.Y. Acad. Sci., 72, 75 (1959).
2. R.H. Wilhelm, A.W. Rice, and A.R. Bendelius, Ind. Eng. Chem., 5, 141 (166).
3. R.L. Pigford, B. Baker, and D.E. Blum, Ind. Eng. Chem. Fundam., 8, 848 (1969).
4. P.C. Wankat, Separ. Sci. 9, 85 (1974).
5. L.C. Craig and D. Craig, in "Technique of Organic Chemistry," Vol. 3, A. Weissberger, ed., Interscience, New York, 1956, pp. 149-332.
6. P.C. Wankat, Separ. Sci., 8, 473 (1973).
7. P.C. Wankat, J. Chromatog., 88, 211 (1974).
8. P.C. Wankat, Ind. Eng. Chem. Fundam. 14, 96 (1975).
9. M.E. Busbice and P.C. Wankat, J. Chromatog. (in press).

10. J.C. Giddings, "Dynamics of Chromatography", Marcel Dekker, N.Y., 1965, pp. 26-35.
11. B. Baker and R.L. Pigford, Ind. Eng. Chem., 10, 283 (1971).
12. R.L. Pigford, B. Baker, D.E. Blum, Ind. Eng. Chem. Fundam., 8, 144 (1969).
13. A.A. Zhukhovitskii, in "Gas Chromatogaphy -- 1960", R.P.W. Scott, ed., Butterworths, London, 1960, pp. 293-300.
14. R. Gupta and N.H. Sweed, Ind. Eng. Chem. Fundam., 9, 21 (1970).
15. D. Meir and R. Lavie, Chem. Eng. Sci., 29, 1133 (1974).
16. E. Van der Vlist, Separ. Sci., 6, 727 (1972).
17. V.R. Ginde and C. Chu, Desalination, 10, 209 (1972).
18. M.E. Busbice, M.S. Thesis, Purdue University, 1974.

NOMENCLATURE

The nomenclature used for the local equilibrium theory follows that of Baker and Pigford[11]. The nomenclature for the staged equilibrium theory follows that of Wankat[8]. The essential parts of these nomenclatures are repeated below.

Local Equilibrium Theory

A = Solid-fluid equilibrium distribution parameter, units depend on function

D_m = mass molecular diffusivity, cm^2/min

D_T = thermal molecular diffusivity, cm^2/min

E_D = eddy axial dispersion, cm^2/min

c = fluid concentration, moles/ℓ

c^* = fluid concentration in equilibrium with wolid phase concentration, moles/ℓ

h = heat transfer coefficient, $cal/(cm^2)(min)(°C)$

k = exponent in Freundlich isotherm

C = heat capacity, cal/(gm)(°C)

T = temperature °C

L = length of bed, cm

q = solid-phase concentration, mol/kg of dry solid

t = time, min

v = interstitial fluid velocity, cm/min

z = axial distance, cm

Greek Letters

α = interparticle void fraction

ϵ = intraparticle void fraction

μ = wave velocity, cm/min

ρ_s = structural density of solid, kg/cm^3

ρ_f = fluid density, kg/cm^3

α_{AV} = average separation factor

Subscripts

C = cold

H = hot

c = concentration related

s = solid

th = thermal

1,2,3 = refer to conditions at temperatures T_1, T_2, T_3

f = feed condition

w = tube wall surroundings

Superscripts

C = cold

H = hot

Equilibrium Staged Theory

A = thermal wave velocity defined by eq. 9

C_{PM}, C_{PS}, C_{PT} = thermal conductivities of mobile phase, solid phase and tube or column wall, cal/g°C

K = distribution coefficient = conc solute in mobile phase/conc solute in stationary phase.

M = mass of solute in stage, g

T = temperature, °C

V_M, V_S = volume of mobile and stationary phases per stage, ml

f = fraction of solute in mobile phase, defined by eq. 10

ρ_M, ρ_S = densities of mobile and solid phases, g/ml

Subscripts

A,B,C = components A,B,C

i = number of stage

S = transfer step number

S_C, S_1, S_2, S_3 = number of transfer steps at temperatures, T_C, T_1, T_2, T_3